

## Two-dimensional self-patterning of PbTiO<sub>3</sub> on a Nb–SrTiO<sub>3</sub> (001) surface using atomic force microscope lithography and hydrothermal epitaxy

R. H. Kim, W. S. Ahn, S. H. Han, and S. K. Choi<sup>a)</sup>

Department of Materials Science and Engineering, Korea Advanced Institute of Science and Technology, 373-1 Guseong-Dong, Yuseong-Gu, Daejeon 305-701, Republic of Korea

(Received 30 October 2006; accepted 29 March 2007; published online 25 April 2007)

Atomic force microscope (AFM) lithography and hydrothermal epitaxy processes were used to resolve issues related to aligning ferroelectric micro- and nanosized cell arrays through a bottom-up approach. A Nb-doped SrTiO<sub>3</sub> (100) surface was transformed in two dimensions by applying bias using a conductive AFM tip. The locally transformed areas were etched out with an acidic solution. It was found that the PbTiO<sub>3</sub> crystal nucleated and grew on the artificially aligned grooves preferentially during a hydrothermal epitaxial process. The self-patterned PbTiO<sub>3</sub> cell had excellent piezoresponse hysteresis with ferroelectric properties suitable for the fabrication of micro- and nanosized ferroelectric devices. © 2007 American Institute of Physics. [DOI: 10.1063/1.2732175]

Ferroelectric thin films with a perovskite structure have been studied for applications such as ferroelectric random access memory and micropiezoelectric sensors and actuators.<sup>1,2</sup> In order for these thin films to be more feasible in micro- and nanosized devices, the ferroelectric materials should be two-dimensionally arrayed using either a top-down or bottom-up approach.<sup>3</sup> The former approach, as conventionally used, entails unavoidable disadvantages including damage to the sidewalls and boundary lines of the ferroelectric cells.<sup>4</sup> Thus, it is difficult to determine the true intrinsic ferroelectric size effects for high density memory devices. On the other hand, the bottom-up method is based on building structures by growing self-aligned cells without a post-patterning process.<sup>5</sup> Therefore, this process has an important benefit in that no mechanical damage is caused if using it. However, thus far this approach does not fully address all issues related to a two-dimensional (2D) array for ferroelectric cells. Moreover, both the top-down and bottom-up approaches require a high-temperature heat treatment above the phase transition temperature ( $T_c$ ) in order to transform the intermediate pyrochlore structure into a ferroelectric perovskite structure.<sup>6,7</sup> This high-temperature process can lead to thermal stress, lead or oxygen vacancies, interdiffusion between the ferroelectric cell and substrate, and the occurrence of polydomain structures. Such defects drastically reduce the ferroelectric and piezoelectric effects of nanoferroelectric devices.<sup>8</sup>

Since chemical modification of hydrogen-passivated *n*-type Si (111) surfaces was induced by a scanning tunneling microscope operating in air,<sup>9</sup> atomic force microscope (AFM) lithography has become a viable alternative for the fabrication of nanoscaled patterns and devices. It has also been performed on semiconducting oxygen deficient SrTiO<sub>3- $\delta$</sub>  films and Nb-doped SrTiO<sub>3</sub> crystal surfaces.<sup>10,11</sup> When the voltage is applied on a solid surface through a conductive AFM tip, the contact area of the surface with the tip is chemically transformed under an ambient humidity. The AFM lithography process is completed when the chemically transformed local area is chemically etched in an acidic solution such as HF or HCl. For metal and silicon surfaces,

the transformation phenomena caused by a conductive AFM tip can be understood in terms of the electrochemical oxidation.<sup>12</sup> However, for other complicated materials such as doped strontium titanate<sup>10,11</sup> and La<sub>0.67</sub>Ba<sub>0.33</sub>MnO<sub>3</sub> film,<sup>13</sup> the phenomena are not yet clear.

Hydrothermal epitaxy is a technique that uses aqueous chemical reactions to synthesize inorganic materials under an elevated pressure (<15 MPa) and at a low temperature.<sup>6,14,15</sup> Recently, Jung *et al.* synthesized a heteroepitaxial PbTiO<sub>3</sub> (hereafter PT) film with a +*c* monodomain and a good *P-E* hysteresis on a Nb-doped (100) SrTiO<sub>3</sub> (NSTO) substrate using hydrothermal epitaxy at 160 °C below  $T_c$  (=490 °C).<sup>16</sup> They suggested that the tetragonal PT film was directly formed on the substrate without undergoing a phase transition from a cubic paraelectric to a tetragonal ferroelectric. In the present study, both AFM lithography and hydrothermal epitaxy are used to solve the problem of a 2D alignment of micro- and nanosized ferroelectric cells using a bottom-up approach. It was confirmed that the pattern lithographed on a NSTO (100) surface using AFM was the preferred nucleation site of a ferroelectric cell during a hydrothermal epitaxy process.

Conventionally, two types of termination layers, a SrO and a TiO<sub>2</sub> plane, coexist on the NSTO (100) surface via mechanochemical polishing. However, treatment with a buffered NH<sub>4</sub>F–HF solution (BHF) forces the NSTO (100) surface to terminate with the TiO<sub>2</sub> plane.<sup>17</sup> Furthermore, if the surface is miscut against the (100) plane, the surface undergoes a stepped TiO<sub>2</sub> termination after the high-temperature annealing treatment. It was also demonstrated that well regulated epitaxy was confirmed by using BHF-treated substrate for the heteroepitaxy of perovskite oxides.<sup>18</sup> Jung *et al.* fabricated a heteroepitaxial PT film with a stepped TiO<sub>2</sub> termination of NSTO.<sup>16</sup> In the present study, a (100) miscut NSTO surface was treated with two different solutions: BHF (for 30 s) and KOH (for 1 min). The substrates were annealed at 1000 °C, for 1 h in an O<sub>2</sub> atmosphere. With these treatments, a stepped morphology was observed in both NSTO (100) surfaces (step height: ~4 Å, terrace width: ~250 nm). The procedure outlined in the next paragraph was conducted on the two types of substrate surfaces.

<sup>a)</sup>Electronic mail: sikchoi50@kaist.ac.kr

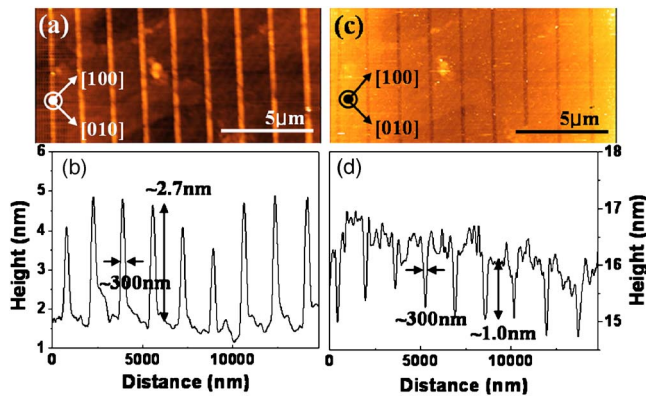


FIG. 1. (Color online) (a) AFM image and (b) line profile of the protrusions at +28 V at the bottom NSTO substrate with  $2\ \mu\text{m}$  intervals; (c) AFM image and (d) line profile of the grooves after etching with a 40% HCl solution.

The AFM lithography process used here is identical to the process reported in Pellegrino *et al.*<sup>10</sup> The bias voltage at the bottom of the stepped NSTO crystal was altered from +20 to +32 V at atmospheric pressure and room temperature. The AFM tip (Ti–Pt coated  $\text{SiN}_x$  tip, spring constant: 14.5 N/m) was scanned at a constant speed of  $0.75\ \mu\text{m}/\text{s}$ . Other parameters, including the humidity (approximately 40%), force reference (zero), and crystal thickness (0.5 mm), were fixed. Thereafter, the NSTO crystals were dipped into a 40% HCl solution for 30 min. After AFM lithography, the NSTO crystal underwent a hydrothermal epitaxy process ( $200\ ^\circ\text{C}$ , 1 h). Detailed conditions of this process are described in the literature.<sup>16</sup>

Figure 1(a) shows a typical AFM image in which electrochemically transformed lines are revealed on both the KOH- and BHF-treated NSTO (100) surfaces when scanned with the AFM tip with a bias voltage of +28 V. As shown in the line profile in Fig. 1(b), the transformed lines protrude with heights of 2–3 nm and a width of  $\sim 300\ \text{nm}$  at  $2\ \mu\text{m}$  intervals between the lines. Figures 1(c) AFM image) and 1(d) (line profile) clearly reveal that the protruding lines are engraved to  $\sim 1\ \text{nm}$  in depth and  $\sim 300\ \text{nm}$  in width after etching with the HCl solution. These results are identical to those reported in a previous study.<sup>10</sup> However, it is expected that the grooves act as preferential nucleation sites during the self-patterning of PT cells.

Before the KOH- and BHF-treated NSTO (100) surfaces were AFM lithographed, they directly underwent a batch of hydrothermal processes, as reported in Ahn *et al.*<sup>19</sup> The results are shown in the scanning electron microscopy (SEM) surface image shown in Fig. 2(a) (KOH treated) and the inset (BHF treated). It can be seen in Fig. 2(a) that the nucleation and growth of the PT islands were mostly suppressed by the KOH treatment. However, PT islands nucleate and grow on the BHF-treated surface, as shown in the inset of that figure. This dissimilar behavior was the impetus for further experiments. A KOH-treated surface with  $5\ \mu\text{m}$  interval patterned grooves underwent a hydrothermal epitaxy process; a SEM surface image of this result is shown in Fig. 2(b). As was expected, the PT lines form mainly on the grooves. However, several PT islands were observed on the original surface (see arrow). Thus, it appears that this unwanted PT island nucleates on the etching pit during the hydrothermal process. For this reason, it is very important to suppress the nucleation of

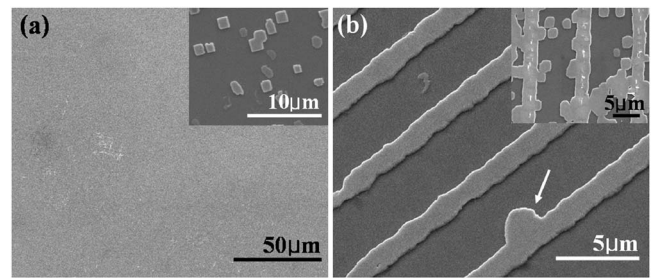


FIG. 2. (a) SEM images of no  $\text{PbTiO}_3$  islands grown on the KOH-treated NSTO substrate;  $\text{PbTiO}_3$  islands on the BHF-treated substrate in the respective inset. (b) SEM image of 2D self-aligned  $\text{PbTiO}_3$  cells grown on the grooves of the KOH-treated substrate after the hydrothermal epitaxial process. The inset of (b) shows an unsuccessful alignment of  $\text{PbTiO}_3$  lines on the BHF-treated substrate after the hydrothermal epitaxy process.

PT cells on the etching pit. The width and thickness of the aligned lines are  $\sim 2.2\ \mu\text{m}$  and  $\sim 150\ \text{nm}$ , respectively, and the interval between the lines is  $5\ \mu\text{m}$ , which is identical to the groove interval. In contrast, with the BHF-treated surface, many PT islands nucleated and grew on the original  $\text{TiO}_2$  surface, as shown in the inset of Fig. 2(b). Thus, the alignment of the PT cells was not successful.

The nucleation from crack and the surface step edge should occur very easily compared to the use of a microscopically flat surface.<sup>20</sup> The KOH-treated NSTO (100) surface also has surface steps. It appears that this surface step is not an effective nucleation site for a PT island. If the NSTO surface reacts with a basic solution such as KOH, a  $\text{SrO}_x$ -rich termination would be obtained. It is expected that the  $\text{SrO}_x$ -rich termination would increase the activation energy for PT nucleation on the surface step edge. On the other hand, the PT island nucleates and grows on the AFM lithographed grooves. Two possible scenarios can be considered. The first is that  $\text{TiO}_2$  rich termination appears on the groove surface ( $\sim 1\ \text{nm}$  groove depth). Additionally, the groove has an  $\sim 300\ \text{nm}$  surface width; thus, a PT island nucleates easily on the groove edge (or the  $\text{TiO}_2$  surface). The second scenario simply involves the difference between the surface step height ( $\sim 0.4\ \text{nm}$ ) and the groove edge depth ( $\sim 1\ \text{nm}$ ). It is also expected that the deeper step depth effectively decreases the activation energy for the nucleation of the PT island. More detailed experimental and analytical studies are required in order to understand the preferential nucleation of a PT island on the AFM lithographed groove of a KOH-treated NSTO (001) surface.

The ferroelectric properties of the PT lines were confirmed using piezoresponse force microscopy (PFM), and the results are shown in Fig. 3. From the PFM image in Fig. 3(a), the PT lines reveal only a positive piezoresponse signal in the as-fabricated state which indicates that the PT lines have only a +*c* monodomain, as the polarization vector directs toward the surface from the interface.<sup>21,22</sup> A +*c* monodomain structure in the hydrothermally synthesized PT film was reported by Jung *et al.*; however, the origin of the +*c* monodomain is not yet clear.<sup>16</sup> The unwanted PT island is also seen in this figure (see arrow). The inset in Fig. 3(a) shows the characters of “NRL” written using the proposed AFM lithography and the hydrothermal epitaxy process. Figure 3(b) represents a typical piezoresponse hysteresis curve of a PT line measured using a conductive AFM tip. The curve clearly shows that polarization switching of the *c* monodomain occurs sharply, which gives the lines excellent

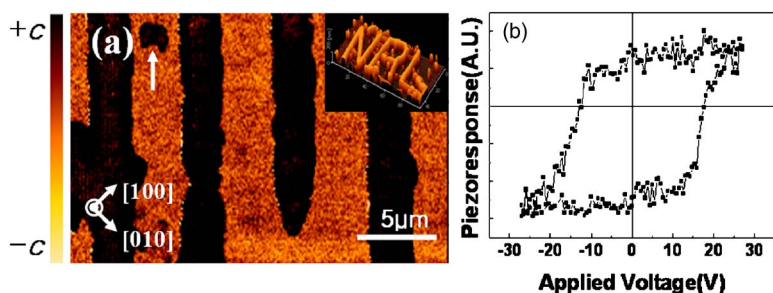


FIG. 3. (Color online) (a) PFM image and (b) piezoresponse hysteresis curve of 2D aligned  $\text{PbTiO}_3$  cells having  $a+c$  monodomain in the as-fabricated state. The inset of (a) demonstrates the characters “NRL” written using the AFM lithography process and hydrothermal epitaxy in this study.

ferroelectric properties. However, the curve is positively biased. This shows an imprint phenomenon that may be related to a  $+c$  monodomain structure in the as-fabricated state.

Ahn *et al.* reported that a  $\text{Pt/PbZr}_{(1-x)}\text{Ti}_x\text{O}_3$  (PZT)/NSTO capacitor in which a heteroepitaxial PZT film was fabricated by hydrothermal epitaxy revealed fatigue-free behavior until  $10^{11}$  fatigue cycles.<sup>23</sup> It is believed that this fatigue behavior results from the good crystal quality of the heteroepitaxial PZT film, as the hydrothermally synthesized PZT film does not have defects such as oxygen vacancies. It is generally believed that fatigue behavior in a perovskite ferroelectric capacitor with Pt electrodes is due to oxygen vacancies in the perovskite ferroelectric film.<sup>24</sup> Therefore, it is expected that  $\text{PbTiO}_3$  lines fabricated by AFM lithography and hydrothermal epitaxy [Fig. 2(b)] would have a good crystal quality for micro- and nanosized devices.

In summary, this study showed that ferroelectric  $\text{PbTiO}_3$  cells can be 2D self-arrayed on artificially produced nucleation sites using AFM lithography. By biasing the conductive AFM tip, the local area of the NSTO (100) surface was transformed electrochemically and the transformed area was etched out with an acidic solution. The grooves provided nucleation sites to grow 2D self-patterned  $\text{PbTiO}_3$  lines during a hydrothermal epitaxy process. The 2D self-patterned  $\text{PbTiO}_3$  lines in this study have an excellent piezoresponse hysteresis, showing that it has suitable ferroelectric properties for applications to micro- and nanosized ferroelectric devices.

This work was supported by the Korea Science and Engineering Foundation (KOSEF) through the National Research Laboratory Program funded by the Ministry of Science and Technology (No. M10400000024-04J0000-02410).

<sup>1</sup>J. F. Scott and C. A. Araujo, *Science* **246**, 1400 (1989).

<sup>2</sup>P. Murali, A. Kholkin, M. Kohli, and T. Meader, *Sens. Actuators, A* **53**, 398 (1996).

<sup>3</sup>M. Alexe, C. Harnagea, and D. Hesse, *J. Electroceram.* **12**, 69 (2004).

<sup>4</sup>S. Clemens, T. Schnell, A. Hart, F. Peter, and R. Waser, *Adv. Mater. (Weinheim, Ger.)* **17**, 1357 (2005).

<sup>5</sup>I. Szafraniak, C. Harnagea, R. Scholz, S. Bhattacharyya, D. Hesse, and M. Alex, *Appl. Phys. Lett.* **83**, 2211 (2003).

<sup>6</sup>F. F. Lange, *Science* **273**, 903 (1996).

<sup>7</sup>A. D. Poli, F. F. Lange, and C. G. Levi, *J. Am. Ceram. Soc.* **83**, 873 (2000).

<sup>8</sup>M. W. Chu, I. Szafraniak, R. Scholz, C. Harnagea, D. Hesse, M. Alexe, and U. Gösele, *Nat. Mater.* **3**, 87 (2004).

<sup>9</sup>J. A. Dagata, J. Schneir, H. H. Harary, C. J. Evans, M. T. Postek, and J. Bennet, *Appl. Phys. Lett.* **56**, 2001 (1990).

<sup>10</sup>L. Pellegrino, I. Pallecchi, D. Marré, E. Bellingeri, and A. S. Siri, *Appl. Phys. Lett.* **81**, 3849 (2002).

<sup>11</sup>R.-W. Li, T. Kanki, M. Hirooka, A. Takagi, T. Matsumoto, H. Tanaka, and T. Kawai, *Appl. Phys. Lett.* **84**, 2670 (2004).

<sup>12</sup>H. Sugimura and N. Nakagiri, *J. Vac. Sci. Technol. A* **14**, 1223 (1996).

<sup>13</sup>I. Pallecchi, L. Pellegrino, E. Bellingeri, A. S. Siri, and D. Marré, *Appl. Phys. Lett.* **83**, 4435 (2003).

<sup>14</sup>A. T. Chien, J. Sachleben, J. H. Kim, J. S. Speck, and F. F. Lange, *J. Mater. Res.* **14**, 3303 (1999).

<sup>15</sup>A. T. Chien, X. Xu, J. H. Kim, J. S. Speck, and F. F. Lange, *J. Mater. Res.* **14**, 3330 (1999).

<sup>16</sup>W. W. Jung, H. C. Lee, W. S. Ahn, S. H. Ahn, and S. K. Choi, *Appl. Phys. Lett.* **86**, 252901 (2005).

<sup>17</sup>M. Kawasaki, K. Takahashi, T. Maeda, R. Tsuchiya, M. Shinohara, O. Ishiyama, T. Yonezawa, M. Yoshimoto, and H. Koinuma, *Science* **266**, 1540 (1994).

<sup>18</sup>M. Kawasaki, A. Ohtomo, T. Arakane, K. Takahashi, M. Yoshimoto, and H. Koinuma, *Appl. Surf. Sci.* **107**, 102 (1996).

<sup>19</sup>S. H. Ahn, W. W. Jung, and S. K. Choi, *Appl. Phys. Lett.* **86**, 172901 (2005).

<sup>20</sup>D. A. Porter and K. E. Easterling, *Phase Transformations in Metals and Alloys* (Van Nostrand Reinhold, New York, 1981), pp. 196–197.

<sup>21</sup>A. Gruverman, O. Auciello, R. Ramesh, and H. Tokumoto, *Nanotechnology* **8**, A38 (1997).

<sup>22</sup>L. M. Eng, *Nanotechnology* **10**, 405 (1999).

<sup>23</sup>W. S. Ahn, W. W. Jung, and S. K. Choi, *J. Appl. Phys.* **99**, 014103 (2006).

<sup>24</sup>J. F. Scott, C. A. Araujo, B. M. Melnick, L. D. Mcmillan, and R. Zuleeg, *J. Appl. Phys.* **70**, 382 (1991).